

# Optical and Structural Properties of ZnO Thin Films Fabricated by Sol-Gel Method

Ziaul Raza Khan<sup>1</sup>, Mohd Shoeb Khan<sup>2</sup>, Mohammad Zulfequar<sup>1</sup>, Mohd Shahid Khan<sup>1\*</sup>

<sup>1</sup>Department of Physics, Jamia Millia Islamia, New Delhi, India; <sup>2</sup>Department of Chemistry, Jamia Millia Islamia, New Delhi, India.  
Email: Shahidkhan\_m@yahoo.com

Received January 24<sup>th</sup>, 2011; revised February 10<sup>th</sup>, 2011; accepted March 15<sup>th</sup>, 2011.

## ABSTRACT

Highly oriented and transparent ZnO thin films have been fabricated on ultrasonically cleaned quartz substrates by the sol-gel technique. X-ray diffraction, UV-VIS, FTIR, photoluminescence and SEM are used to characterize ZnO thin films. X-ray diffraction study show that all the films prepared in this work have hexagonal wurtzite structure, with lattice constants  $a = b = 3.260 \text{ \AA}$ ,  $c = 5.214 \text{ \AA}$ . The optical band gap energy of the thin films is found to be direct allowed transition  $\sim 3.24 \text{ eV}$ . The FTIR spectrum of the film has the characteristics ZnO absorption band at  $482 \text{ cm}^{-1}$ . The photoluminescence spectrum of the samples has an UV emission peak centred at  $383 \text{ nm}$  with broad band visible emission centred in the range of  $500 - 600 \text{ nm}$ .

**Keywords:** ZnO, XRD, SEM, Photoluminescence, Band Gap

## 1. Introduction

Significant research efforts have been made in recent years for developing highly oriented and transparent ZnO thin films, because of their potential application in transparent electrode in display, window layers in solar cells, field emitters, ultraviolet laser emission, photodetectors, piezoelectricity, bio-sensors, short wavelength light emitting diode and information technology [1-8]. A II-VI group semiconductor material ZnO has wide band gap ( $\sim 3.3 \text{ eV}$  at room temperature) and large excitonic binding energy  $\sim 60 \text{ meV}$ . Due to their unique optical, electrical and semiconducting properties, ZnO thin films are extensively used in various applications. Despite several approaches adopted for making these ZnO thin films; controlling the size, shape, crystallinity and various parameters affecting the size and shape of these materials still need to be investigated. Therefore, it is essential to investigate optimum conditions for fabrication of highly oriented and transparent ZnO thin films. The main concern of researcher is to get better quality of material stoichiometry. ZnO thin films are grown by different techniques such as pulsed laser deposition (PLD), magnetron sputtering, MOCVD, spray pyrolysis etc [9-12]. Sol-gel technique is widely adopted due to its comparatively simple procedure as there is no need of costly vacuum system and it has a wide-range advantage

of large area deposition and uniformity of the films thickness. The sol-gel process also offers other advantages for thin film deposition including outstanding control of the stoichiometry and easy doping in film composition. The structural and physical properties of ZnO thin films prepared by sol-gel technique using various inorganic and organic precursors at different deposition conditions have been reported in literature [13,14]. In the present work, we report growth of ZnO thin films on quartz substrate by Sol-gel method using zinc acetate precursor and their structural, optical, vibrational and photoluminescence properties.

## 2. Experimental Details

All the reagents used in the present work for the chemical synthesis were of analytical grade. Zinc acetate dihydrate ( $\text{Zn}(\text{CH}_3\text{COO})_2 \cdot 2\text{H}_2\text{O}$ ) was first dissolved in a 2-methoxyethanol ( $(\text{CH}_3)_2\text{CHOH}$ ) with monoethanolamine (MEA:  $\text{H}_2\text{NCH}_2\text{CH}_2\text{OH}$ ) which was used as a stabiliser. The molar ratio of MEA to zinc acetate was kept to 1.0 and concentration of zinc acetate was  $0.80 \text{ mol/l}$ . The resultant solution was stirred at  $60^\circ\text{C}$  for 1 h to yield a clear and homogeneous solution ready for coating. The coating was performed with freshly prepared solution. The films on ultrasonically cleaned quartz substrates were prepared using spin-coating unit which was rotated at  $3000 \text{ rpm}$  for  $30 \text{ s}$ . The films were preheated (baked)

at temperature 250°C for 5 min in a furnace to evaporate the solvent and remove organic residuals. The spin-coating to preheating procedure was repeated ten times. The films were then post-heated (annealed) in air at 400°C for three hour. The phases of ZnO thin film were determined by X-ray diffraction, using Panalytical Diffractometer type PW3710 with Cu Ka radiation ( $\lambda = 0.154$  nm). Optical transmittance was observed using UV-Visible double beam spectrophotometer model (Jasco-V570), and the optical band gap energy was calculated from the data of the optical transmittance and wavelength. The IR spectrum was recorded using SHIMADZU FTIR-8400S Japan in the range of 400  $\text{cm}^{-1}$  to 5000  $\text{cm}^{-1}$ . Photoluminescence of the samples was measured using a He-Cd laser as an excitation source, operating at 325 nm with an output power of 50 mW and monochromatic (Jovin Youvan) fitted with a Hamamatsu R928 photomultiplier detector. Surface morphology was examined by the Scanning Electron Microscope model-Carl ZEISS EVO-40.

### 3. Results and Discussion

#### 3.1. X-Ray Diffraction Analysis

The XRD pattern of ZnO thin film fabricated by sol-gel method on quartz substrates is shown in **Figure 1**. All the peaks of the ZnO thin films correspond to the peaks of standard ZnO (JCPDS S6-314). For all the samples, (100), (101) and (002) diffraction peaks are observed in the XRD pattern, showing the growth of ZnO crystallites along different directions. Strong preferential growth is observed along (002) plane indicating that the films are oriented along c-axis [6]. The typical hexagonal wurtzite structure of thin films is inferred from the XRD pattern.

The crystallites sizes (D) of the films are estimated using the Scherer formula [15]:

$$D = \frac{k\lambda}{\beta_{2\theta} \cos \theta} \quad (1)$$

where  $k$  is a constant taken to be 0.94,  $\lambda$  is the wavelength of X-Ray used ( $\lambda = 1.54$  Å) and  $\beta_{2\theta}$  is the full width at half maximum of (002) peak of XRD pattern, Bragg angle,  $2\theta$ , is around 34.44°. The average value of grain size is found to be 20 nm.

The dislocation density ( $\delta$ ), defined as the length of dislocation lines per unit volume, are estimated using the equation:

$$\delta = \frac{1}{D^2} \quad (2)$$

Strain ( $\varepsilon$ ) of the thin films is estimated using the equation:

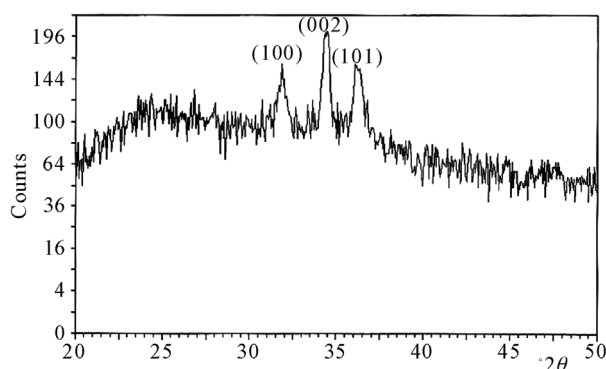


Figure 1. XRD pattern of ZnO thin film.

$$\varepsilon = \frac{\beta \cos \theta}{4} \quad (3)$$

The evaluated structural parameters of thin films are presented in **Table 1**.

The lattice parameters of ZnO thin films evaluated from XRD data are in good agreement with those reported in (JCPDS S6-314). The calculated lattice parameters are given in **Table 2**.

#### 3.2. Optical Properties

The optical transmission spectrum of the ZnO thin film grown on quartz substrates is shown in **Figure 2**. The average value of transmittance of thin films in the visible range is found to be 91% - 95%. In the visible region of solar spectrum, transmission spectra of ZnO thin films show sinusoidal behaviour; this may be due to the layered structure of thin films. The value of band gap is estimated from fundamental absorption edge of the films. For the direct transitions, the absorption coefficient is expressed by [16]:

$$(\alpha hv) = A(hv - E_g)^{1/2} \quad (4)$$

where  $A$  is the constant,  $E_g$  is the energy gap,  $\nu$  is the frequency of the incident radiation and  $h$  is Planck's constant. **Figure 3** shows the plot  $(\alpha hv)^2$  vs.  $hv$ . The  $E_g$  values of thin film are calculated from this plot. The presence of a single slope in the plot suggests that the films have direct and allowed transition. The band gap energy is obtained by extrapolating the straight line portion of the plot to zero absorption coefficient. The band gap value of ZnO thin film is found to be 3.24 eV.

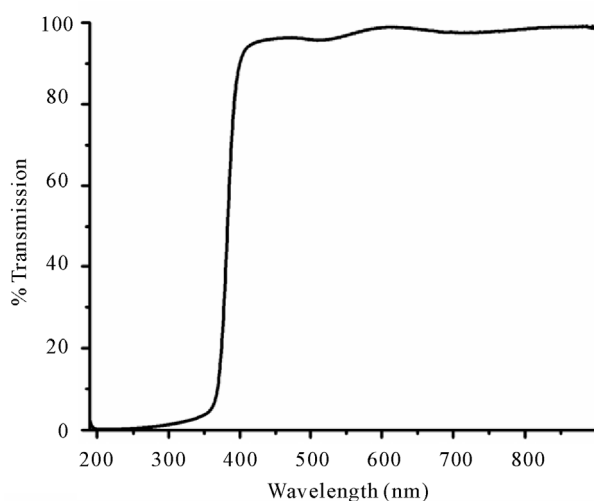
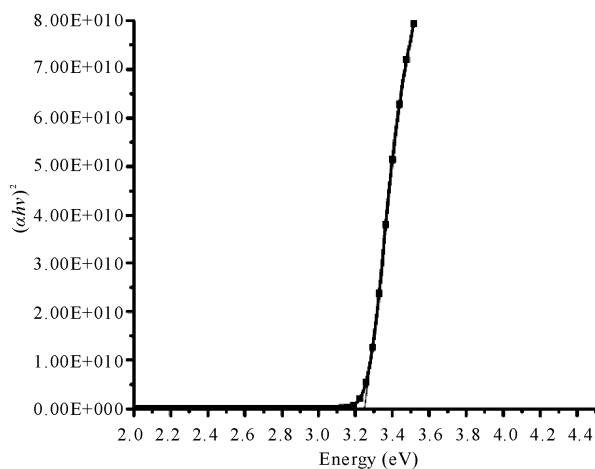
The absorption coefficient of ZnO thin films is shown in **Figure 4**. The absorption coefficient of ZnO thin films is found to be zero in forbidden energy region and it is found to increase rapidly with the decrease in wavelength beyond energy band gap. Zero absorption coefficients of ZnO thin films in the visible range of spectrum make these thin films suitable as window layer in solar cells.

**Table 1. Structural parameters of ZnO thin films.**

Planes	Interplanar spacing( $\text{\AA}$ ) d (002)	FWHM( $\beta$ ) (002) ( $\times 10^{-3}$ (rad.))	Grain size D (nm)	$\delta$ ( $\times 10^{14}$ ) (lines/m <sup>2</sup> )	$\varepsilon$ ( $\times 10^{-3}$ )
(100)	2.8095	8.37	18	30.86	2.01
(002)	2.6016	6.28	24	17.36	1.49
(101)	2.4764	8.37	18	30.86	1.98

**Table 2. Lattice parameters of the ZnO thin film.**

$a$ ( $\text{\AA}$ )		$c$ ( $\text{\AA}$ )	
Calculated	Standard	Calculated	Standard
3.260	3.253	5.214	5.215

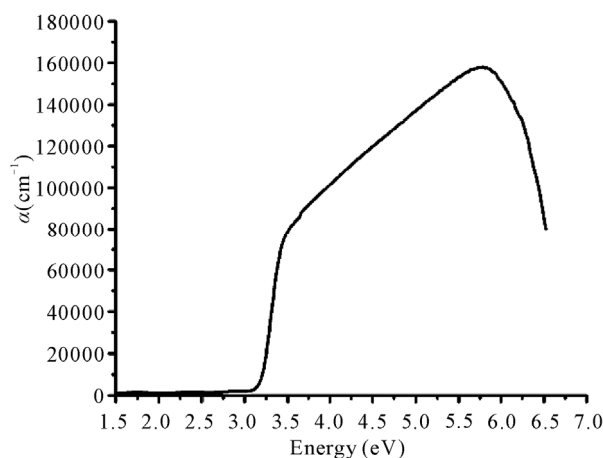
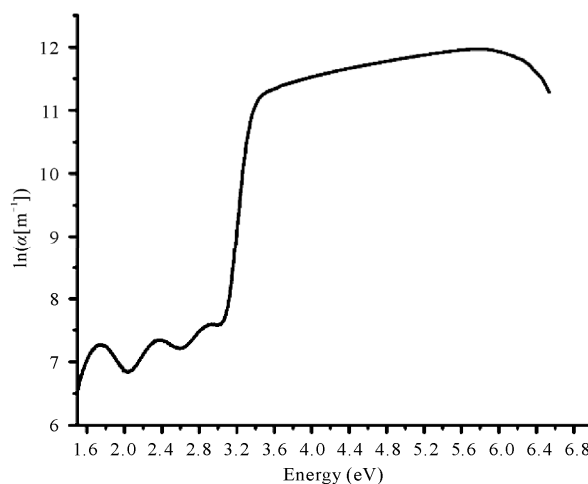
**Figure 2. Transmission spectrum of ZnO thin film.****Figure 3. The plots  $(ah\nu)^2$  vs. photon energy of the ZnO thin film.**

The logarithm of the absorption coefficient  $\alpha(\nu)$  of ZnO thin films is plotted as a function of the photon en-

ergy ( $h\nu$ ) in **Figure 5**. The values of the Urbach's energy ( $E_u$ ) are calculated by taking the reciprocal of the slopes of the linear portion in the lower photon energy region of these curves and the value of Urbach energy found to be 0.06 eV. Urbach energy  $E_u$  is very important tools to investigate structural disorder in thin films as reported by M. Caglar *et al.* in [16].

### 3.3. FTIR Analysis

FTIR spectroscopy is very useful tools for investigating

**Figure 4. The plots  $\alpha$  vs. energy of ZnO thin film.****Figure 5. The plots of  $\ln(\alpha)$  vs. photon energy of ZnO thin film.**

vibrational properties of synthesized materials. The band positions and absorption peak not only depend on the chemical composition and structure of the thin films but on the morphology of thin films also [17]. FTIR spectrum of ZnO thin film is shown in **Figure 6**. The absorption band observed at  $482\text{ cm}^{-1}$  is attributed to the ZnO stretching vibrations [18]. The broad peak in the range of  $3900\text{ to }3800\text{ cm}^{-1}$  is attributed to water molecule present in thin films. Weak peaks at  $1550\text{ cm}^{-1}$  and  $1665\text{ cm}^{-1}$  are attributed to symmetric and asymmetric C=O bonds vibrations respectively. The absorption peaks appearing at  $2380\text{ cm}^{-1}$  is due to the absorption of atmospheric  $\text{CO}_2$  by metallic cation [19]. The IR frequencies along with the vibrational assignment for ZnO thin films are given in **Table 3**.

### 3.4. Photoluminescence Spectroscopy

Photoluminescence spectrum of ZnO thin film is shown in **Figure 7**. Two emission peaks is observed in photoluminescence spectrum. A strong peak centred at  $383\text{ nm}$ , near the band edge due to free exciton emission is observed in photoluminescence spectrum. A weak and broad peak centred at  $550\text{ nm}$  is also observed in photoluminescence spectrum [20]. The broad band in the region of  $500\text{ - }600\text{ nm}$ , in photoluminescence spectrum of ZnO thin films is related to the amount of non-stoichiometric intrinsic defects and the same may be due to zinc vacancy in ZnO films as reported Kim *et al.* [21]. It

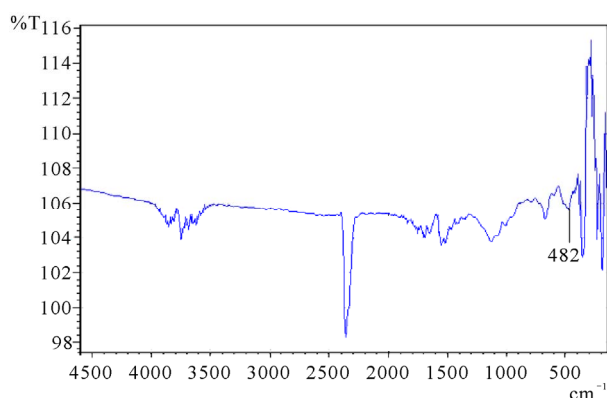


**Figure 6.** FTIR spectrum of ZnO thin film.

**Table 3.** IR frequency assignment with the corresponding bond.

Positions ( $\text{cm}^{-1}$ )	Intensities	Assignments
482	Medium	ZnO stretching
3800, 3900	Doublet	H-O-H stretching
1550, 1665	Doublet	C=O
2380	Strong	O=C=O

is known that pure ZnO can show green or orange visible luminescence depending on the growth temperature and availability of oxygen during sample preparation. The main issue is improving material quality; mostly ZnO shows the ultraviolet emission with the green emission. Visible emission in ZnO shows the defects in material crystal structures. In this thin film we have observed one visible band, presence of this band due to the stoichiometric defects occurs during the synthesis of thin films.

### 3.5. SEM Analysis

Surface morphology of thin films is very important tool to investigate microstructure of thin films. SEM micrograph of ZnO thin films is shown in **Figure 8**. The growth of unsymmetrical ZnO rod having large surface area can be seen in SEM micrograph. From micrograph, it is observed that growth of small square shape crystallites with the rod shape. Such type of square slabs in ZnO thin films are also observed by L. Znaidi *et al.* [12].

## 4. Conclusions

We have grown ZnO thin films on quartz substrates by sol-gel technique with  $0.80\text{ M}$  zinc acetate solutions. Films have been characterized using optical and structural measurements. All the films exhibit high transmittance ( $91\% - 95\%$ ) in the range of  $400\text{ nm}$  to  $800\text{ nm}$ , thus making the films suitable for optoelectronic devices, for instance as window layers in solar cells. The films show a direct transition in the range  $3.24\text{ eV}$ . The X-ray diffraction analysis revealed that all samples have hexagonal wurtzite structure. The crystallites sizes as measured using XRD data are found to be in the range of  $18 - 24\text{ nm}$ . The film has the strong emission band at  $383\text{ nm}$  and also a broad emission peak centred at  $550\text{ nm}$  visible region.

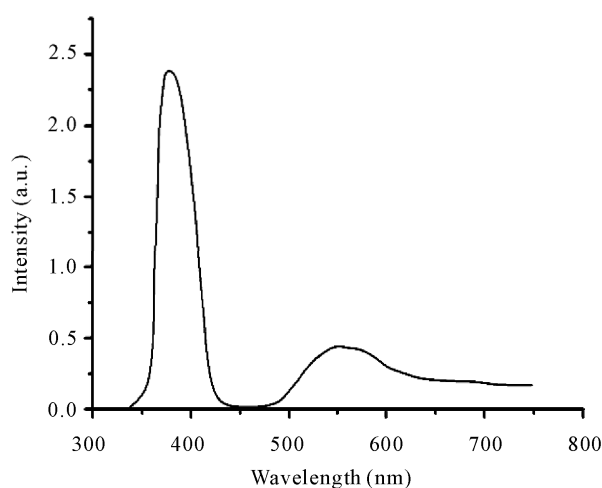


**Figure 7.** Photoluminescence spectrum of ZnO thin film.

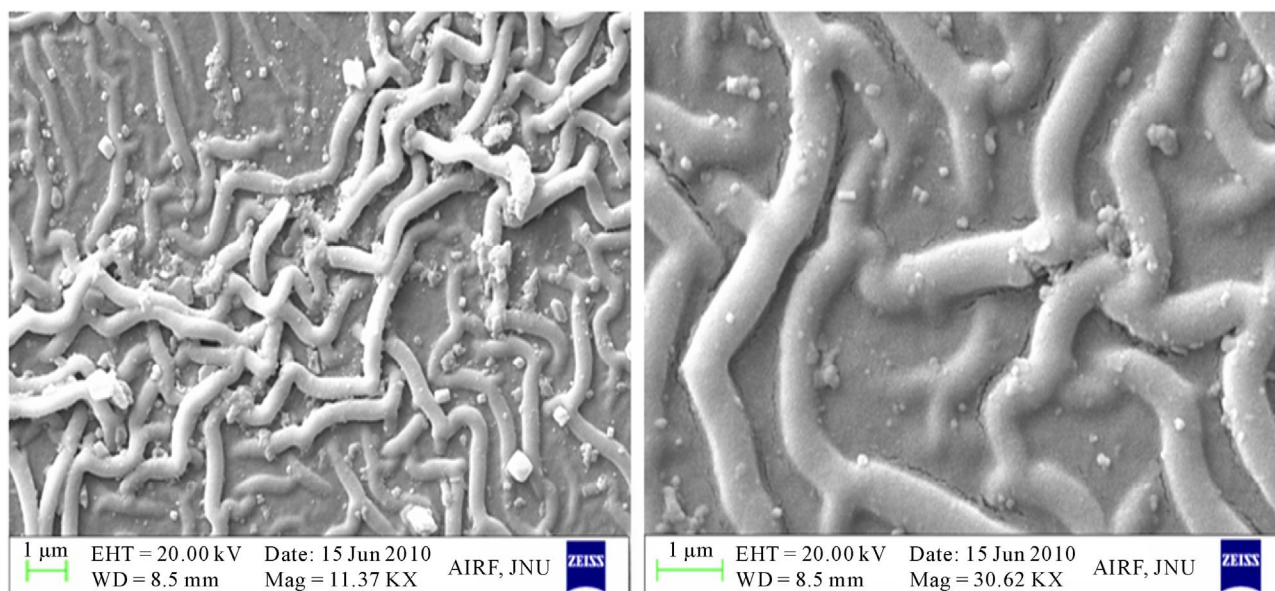


Figure 8. SEM micrograph of ZnO thin film.

## 5. Acknowledgements

The authors are thankful to Material Science Group of National Physical Laboratory, Delhi, India for extending photoluminescence facility.

## REFERENCES

- [1] Z. K. Tang, G. K. L. Wong, P. Yu, M. Kawasaki, A. Ohtomo, H. Koinuma and Y. Segawa, "Room-Temperature Ultraviolet Laser Emission from Self-Assembled ZnO Microcrystallite Thin Films," *Applied Physics Letters*, Vol. 72, No. 25, June 1998, pp. 3270-3272. [doi:10.1063/1.121620](https://doi.org/10.1063/1.121620)
- [2] Y. B. Li, Y. Bando and D. Golberg, "ZnO Nanoneedles with Tip Surface Perturbations: Excellent Field Emitters," *Applied Physics Letters*, Vol. 84, No. 18, May 2004, pp. 3603-3605. [doi:10.1063/1.1738174](https://doi.org/10.1063/1.1738174)
- [3] A. Tsukazaki, A. Ohtomo, T. Onuma, M. Ohtani, T. Mankino, M. Sumiya, K. Ohtani, S. F. Chichibu, S. Fuke, Y. Segawa, H. Koinuma and M. Kawasaki, "Repeated Temperature Modulation Epitaxy for *p*-Type Doping and Light-Emitting Diode Based on ZnO," *Nature Materials*, Vol. 4, No. 1, January 2005, pp. 42-46. [doi:10.1038/nmat1284](https://doi.org/10.1038/nmat1284)
- [4] S. H. Lee, S. S. Lee, J. J. Choi, J. U. Jeon and K. Ro, "Fabrication of a ZnO Piezoelectric Micro Cantilever with a High-Aspect-Ratio Nano Tip," *Microsystem Technologies*, Vol. 11, No. 6, June 2005, pp. 416-423. [doi:10.1007/s00542-004-0494-0](https://doi.org/10.1007/s00542-004-0494-0)
- [5] I. Salaoru, P. A. Buffat, D. Laub, A. Amariei, N. Apetroaei and M. Rusu, "Preparation and Structural Characterization of Thin-Film CdTe/CdS Heterojunctions," *Journal of Optoelectronics and Advanced Materials*, Vol. 8, No. 3, June 2006, pp. 936-940.
- [6] J. Q. Xu, Q. Y. Pan, Y. A. Shun and Z. Z. Tian, "Grain Size Control and Gas Sensing Properties of ZnO Gas Sensor," *Sensors and Actuators B: Chemical*, Vol. 66, No. 1-3, July 2007, pp. 277-279.
- [7] K. J. Chen, F. Y. Hung, S. J. Chang and S. J. Young, "Optoelectronic Characteristics of UV Photodetector Based on ZnO Nanowire Thin Films," *Journal of Alloys and Compounds*, Vol. 479, No. 1-2, June 2009, pp. 674-677. [doi:10.1016/j.jallcom.2009.01.026](https://doi.org/10.1016/j.jallcom.2009.01.026)
- [8] S. Majumdar and P. Bnerji, "Hopping Conduction in Nitrogen Doped ZnO in the Temperature Range 10 - 300 K," *Journal of Applied Physics*, Vol. 107, No. 6, May 2010, pp. 063702-063702-4. [doi:10.1063/1.3353862](https://doi.org/10.1063/1.3353862)
- [9] P. Pushpharajah, S. Radhakrishna and A. K. Arof, "Transparent Conducting Lithium-Doped Nickel Oxide Thin Films by Spray Pyrolysis Technique," *Journal of Materials Science*, Vol. 32, No. 11, June 1997, pp. 3001-3006. [doi:10.1023/A:1018657424566](https://doi.org/10.1023/A:1018657424566)
- [10] J. D. Ye, S. L. Gu, S. M. Zhu, T. Chen, L. Q. Hu, F. Qin, R. Zhang, Y. Shi and Y. D. Zheng, "The Growth and Annealing of Single Crystalline ZnO Films by Low-Pressure MOCVD," *Journal of Crystal Growth*, Vol. 243, No. 1, May 2002, pp. 151-160. [doi:10.1016/S0022-0248\(02\)01474-4](https://doi.org/10.1016/S0022-0248(02)01474-4)
- [11] J. B. Lee, S. H. Kwak and H. J. Kim, "Effects of Surface Roughness of Substrates on the *c*-Axis Preferred Orientation of ZnO Films Deposited by r.f. Magnetron Sputtering," *Thin Solid Films*, Vol. 423, No. 2, January 2003, pp. 262-266. [doi:10.1016/S0040-6090\(02\)00977-X](https://doi.org/10.1016/S0040-6090(02)00977-X)
- [12] L. Znaidi, G. J. A. A. S. Illia, S. Benyahia, C. Sanchez and A. V. Kanaev, "Oriented ZnO Thin Films Synthesis by Sol-Gel Process for Laser Application," *Thin Solid Films*, Vol. 428, No. 1-2, March 2003, pp. 257-262. [doi:10.1016/S0040-6090\(02\)01219-1](https://doi.org/10.1016/S0040-6090(02)01219-1)

- [13] H. Bahadur, A. K. Srivastava, D. Haranath, H. Chander, A. Basu, S. B. Samanta, K. N. Sood, R. Kishore, R. K. Sharma, Rashmi, V. Bhatt, P. Pal and S. Chandra, "Nano-Structured ZnO Films by Sol-Gel Process," *Indian Journal of Pure & Applied Physics*, Vol. 45, April 2007, pp. 395-399.
- [14] H. X. Li, J. Y. Wang, H. Liu, H. J. Zhang and X. Li, "Zinc Oxide Films Prepared by Sol-Gel Method," *Journal of Crystal Growth*, Vol. 275, No. 1-2, February 2005, pp. e943-e946. [doi:10.1016/j.jcrysgro.2004.11.098](https://doi.org/10.1016/j.jcrysgro.2004.11.098)
- [15] Z. R. Khan, M. Zulfeqar and M. S. Khan, "Optical and Structural Properties of Thermally Evaporated Cadmium Sulphide Thin Films on Silicon (100) Wafers," *Materials Science and Engineering: B*, Vol. 174, No. 1-3, October 2010, pp. 145-149. [doi:10.1016/j.mseb.2010.03.006](https://doi.org/10.1016/j.mseb.2010.03.006)
- [16] M. Caglar, S. Ilican and Y. Caglar, "Influence of Dopant Concentration on the Optical Properties of ZnO: In films by Sol-Gel Method," *Thin Solid Films*, Vol. 517, No. 17, July 2009, pp. 5023-5028. [doi:10.1016/j.tsf.2009.03.037](https://doi.org/10.1016/j.tsf.2009.03.037)
- [17] Z. Yang, Z. Z. Ye, Z. Xu and B. H. Zhao, "Effect of the Morphology on the Optical Properties of ZnO Nano-structured," *Physica E: Low-Dimensional Systems and Nanostructures*, Vol. 42, No. 2, December 2009, pp. 116-119. [doi:10.1016/j.physe.2009.09.010](https://doi.org/10.1016/j.physe.2009.09.010)
- [18] T. Ivanova, A. Harizanova, T. Koutzarova and B. Vertruyen, "Study of ZnO Sol-Gel Films: Effect of Annealing," *Materials Letters*, Vol. 64, No. 10, October 2010, pp. 1147-1149. [doi:10.1016/j.matlet.2010.02.033](https://doi.org/10.1016/j.matlet.2010.02.033)
- [19] Y. J. Kwon, K. H. Kim, C. S. Lim and K. B. Shim, "Characterization of ZnO Nanopowders Synthesized by the Polymerized Complex Method via an Organochemical Route," *Journal of Ceramic Processing Research*, Vol. 3, June 2002, pp. 146-149.
- [20] M. Vafaei and M. S. Ghamsari, "Preparation and Characterization of ZnO Nanoparticles by a Novel Sol-Gel Route," *Materials Letters*, Vol. 61, No. 14-15, June 2007, pp. 3265-3268. [doi:10.1016/j.matlet.2006.11.089](https://doi.org/10.1016/j.matlet.2006.11.089)
- [21] Y.-S. Kim, W.-P. Tai, S.-J. Shu, "Effect of Preheating Temperature on Structural and Optical Properties of ZnO Thin Films by Sol-Gel Process," *Thin Solid Films*, Vol. 491, No. 1-2, November 2005, pp. 153-160. [doi:10.1016/j.tsf.2005.06.013](https://doi.org/10.1016/j.tsf.2005.06.013)